ISSN 0511-5728
The West Indian Journal of Engineering
Vol.35, No.2, January 2013, pp.72-82

Identification and Remediation of Water-Quality Hotspots in Havana, Cuba: Accounting for Limited Data and High Uncertainty

Jeffrey J. Iudicello[a Ψ], Dylan A. Batterman[b], Matthew M. Pollard[c], Cameron Q. Scheid[d], and David A. Chin[e]

Department of Civil, Architectural, and Environmental Engineering, University of Miami, Coral Gables, FL, USA
[a] E-mail: jeffrey.iudicello@drbc.state.nj.us
[b] E-mail: d.batterman@umiami.edu
[c] E-mail: m.pollard@wustl.edu
[d] E-mail: c.scheid@umiami.edu
[e] E-mail: dchin@miami.edu

[Ψ] *Corresponding Author*

(Received 19 May 2012; Revised 26 November 2012; Accepted 01 January 2013)

Abstract: *A team at the University of Miami (UM) developed a water-quality model to link in-stream concentrations with land uses in the Almendares River watershed, Cuba. Since necessary data in Cuba is rare or nonexistent, water-quality standards, pollutant data, and stormwater management data from the state of Florida were used, an approach justified by the highly correlated meteorological patterns between South Florida and Havana. A GIS platform was used to delineate the watershed and sub-watersheds and breakdown the watershed into urban and non-urban land uses. The UM model provides a relative assessment of which river junctions were most likely to exceed water-quality standards, and can model water-quality improvements upon application of appropriate remediation strategies. The pollutants considered were TN, TP, BOD_5, fecal coliform, Pb, Cu, Zn, and Cd. The key model result is that the river junctions most likely to exceed water-quality standards are at the intersections of upstream sub-watersheds, and the best way to reduce the concentrations is via better management of the runoff from the upstream sub-watersheds. Dilution and attenuation were significant factors in reducing the concentration at downstream river junctions. The model was conservative in that it did not consider point-sources or groundwater dynamics in the Almendares River, and was found to be comparable to an established USGS water-quality model. The UM model is a valuable tool in assessing the water quality in the Almendares River and can be applied similarly to other rivers in Cuba or in similar countries with water-quality problems and limited data availability.*

Keywords: *Almendares River, water-quality model, infrastructure, Cuba*

1. Introduction

An accurate assessment of the water quality in a stream is of great benefit to society as it reflects the condition of the surrounding natural and man-made environment and can provide warning in case of risk to human health. Normal riverine activities such as bathing and boating, or using the river as a source for drinking water can expose communities to significant risk of illness or fatality if the waters have high toxic or pathogenic content. Likewise, the consumption of fish exposed to toxic substances in the water can greatly increase risk to human health. The conventional approach to managing the quality of water in streams is to control the input of contaminants into the stream from point sources and non-point sources such that applicable water-quality standards are met. However, water-quality problems tend to be greater in lesser-developed countries like Cuba where regulatory standards, relevant scientific data, and enforcement of standards are rare or nonexistent.

To address the problems of limited data and minimal regulations which are particularly prevalent in Cuba, a water-quality model was developed to simulate the effects of stormwater runoff on the stream water quality in the Almendares River watershed, which is home to roughly 2.5 million people and includes the capital city of Havana. Upper and lower portions of the watershed were considered separately, where the runoff was routed from the upper region to the Ejército Rebelde reservoir and from the lower region below the reservoir to the Almendares River's outfall to the sea. The model links land use and runoff to predict in-stream concentrations and assesses uncertainty in light of the significant data limitations. The model identifies the locations in the Almendares River where the greatest water-quality problems are most likely to occur and can predict the water-quality improvements that would result from the implementation of various levels of stormwater control.

The development and application of the model as described in this report can serve as a protocol for

addressing water quality in other parts of Cuba or in similar countries with limited resources and data. The model was developed by a team at the University of Miami (UM) specifically for application to conditions in Cuba and is referred to in this report as the UM model.

2. UM Model

The UM model is formulated for watersheds that contain a network of streams, with each stream segment receiving direct runoff from a sub-area (sub-watershed) within a single overall watershed. Pollutant concentrations are predicted at sub-watershed pour-points from pollutant loads in sub-watershed runoff, where each sub-watershed is divided into "urban" and "non-urban" land uses. The runoff, Q_{sw} (m^3/yr), from each sub-watershed is determined using the relation

$$Q_{sw} = Q_1 + Q_2 = R(C_1A_1 + C_2A_2) \quad (1)$$

where R is the annual rainfall (m), C (dimensionless) and A (m^2) are the runoff coefficient and land area, respectively, and the subscripts 1 and 2 correspond to the urban and non-urban land uses, respectively. The pollutant load in the runoff, L (kg/yr), for each sub-watershed is determined using the relation

$$L = Q_1e_1 + Q_2e_2 = R(C_1A_1e_1 + C_2A_2e_2) \quad (2)$$

where e (typically in mg/L) is the event-mean concentration (EMC) per land use. The average-annual concentration at the pour-point of each sub-watershed, c_{sw}, as shown in Figure 1a is then given by

$$c_{sw} = \frac{L}{Q_{sw}} \quad (3)$$

When stream segments exiting two neighboring sub-watersheds combine at a junction as illustrated in Figure 1b, the streamflows are summed and the average concentration at the junction, c, is determined using a flow-weighted average

$$c = \frac{Q_1c_1 + Q_2c_2 + \sum_{i=1}^{2}(Q_{ui}c_{ai})}{Q_1 + Q_2 + \sum_{i=1}^{2}Q_{ui}} \quad (4)$$

where Q_i and c_i are the flow and concentration in segment i derived from the sub-watersheds contributing directly to segment i, Q_{ui} is the flow entering segment i from an upstream segment, and c_{ai} is the corresponding attenuated concentration from the upstream segment. Figures 1a and 1b show the mass balances for a typical watershed and a junction, respectively.

Attenuation represents the processes by which pollutant concentrations are reduced over the course of a stream segment. The primary attenuation mechanism is sedimentation, where pollutants sorbed to suspended sediment particles are removed as suspended particles settle to the bottom of the stream, thereby reducing the in-stream concentration of the pollutants. The UM model accounted for the attenuation of concentrations from an upstream segment over the length of a downstream segment using the first-order relationship

$$c_a = c_u \exp(-Kx) \quad (5)$$

where c_a is the attenuated concentration at the end of the lower stream segment [ML^{-3}], c_u is the concentration at the end of the upper stream segment [ML^{-3}], K is the attenuation factor [L^{-1}], and x [L] is the length of the downstream segment. The attenuation factor was assumed to be 1000 m^{-1} based on flow rates for certain stream reaches in Havana as stated in Egues and Diaz (1997) and approximate stream dimensions. A sensitivity study and discussion of this assumed value for K are included in a later section.

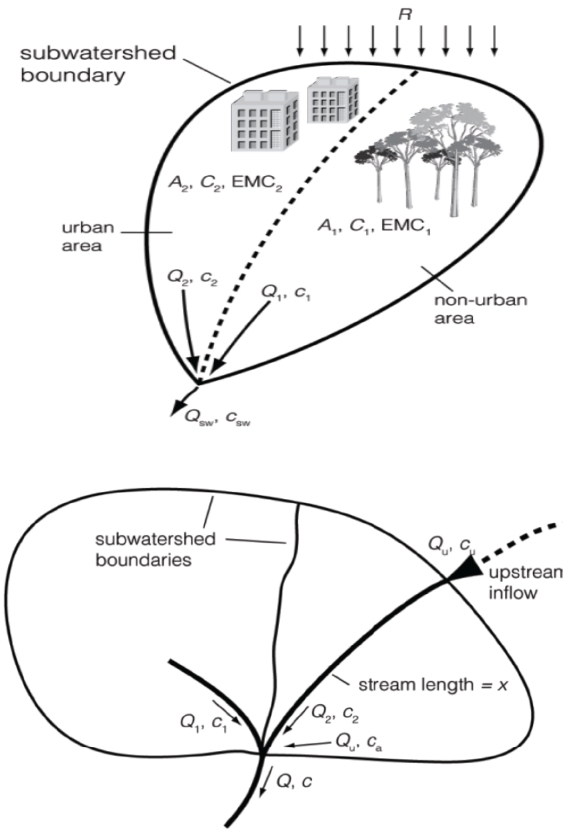

Figure 1b. Mass balances for a junction

2.1 Uncertainty Analysis

An uncertainty analysis was conducted to quantify the uncertainty in model predictions and provide 90%-confidence intervals around average concentrations predicted by the UM model. Due to the natural topography of the Almendares River watershed, the mean and variance of both the flow and concentration contributed by each sub-watershed were found first, then these contributions were combined cumulatively at the downstream junctions where stream segments intersect. Mean flow from each sub-watershed was found using Equation 1 with the averaged value of each variable. The corresponding variance in flow, $\sigma^2_{Q,sw}$, at the exit of a sub-watershed was determined by the first-order relation

$$\sigma_{Q,sw}^2 = (RA_1)^2\sigma_{C_1}^2 + (RA_2)^2\sigma_{C_2}^2 \quad (6)$$

where the subscripts 1 and 2 correspond to urban and non-urban land use, respectively, and $\sigma_{C_1}^2$ and $\sigma_{C_2}^2$ are the variances in the runoff coefficients considered in the model per land use. At each junction, the mean flow leaving the junction is equal to the sum of the average flows entering the junction. The variance in flow leaving the junction, $\sigma_{Q_j}^2$, is the sum of the variances of flows entering the junction

$$\sigma_{Q,j}^2 = \sigma_{Q_1}^2 + \sigma_{Q_2}^2 + \sum_{i=1}^{2}\sigma_{Q_{ui}}^2 \quad (7)$$

where $\sigma_{Q_i}^2$ is the variance in the direct runoff to the i^{th} stream segment, and $\sigma_{Q_{ui}}^2$ is the variance in the flow contributed by the i^{th} upstream segment.

The mean concentration in the runoff from a subwatershed, c_{sw}, was calculated using Equation 3 with mean values of the variables, while at the junctions the mean concentration of the flow leaving the junction is the flow-weighted value given by Equation 4. To determine the variance in the concentration in streams exiting from subwatersheds and junctions, σ_c^2, a first-order second-moment analysis was conducted by using (Benjamin and Cornell, 1970)

$$\sigma_c^2 = \left(\frac{\partial c}{\partial c_1}\right)^2\sigma_{c_1}^2 + \left(\frac{\partial c}{\partial c_2}\right)^2\sigma_{c_2}^2 + \left(\frac{\partial c}{\partial Q_1}\right)^2\sigma_{Q_1}^2 + \left(\frac{\partial c}{\partial Q_2}\right)^2\sigma_{Q_2}^2 \quad (8)$$

where the partial derivatives of c derived from Equation 4 are:

$$\frac{\partial c}{\partial c_1} = \frac{Q_1}{Q_1+Q_2} \quad (9)$$

$$\frac{\partial c}{\partial c_2} = \frac{Q_2}{Q_1+Q_2} \quad (10)$$

$$\frac{\partial c}{\partial Q_1} = \frac{Q_2c_1 - Q_2c_2}{(Q_1+Q_2)^2} \quad (11)$$

$$\frac{\partial c}{\partial Q_2} = \frac{Q_1c_2 - Q_1c_1}{(Q_1+Q_2)^2} \quad (12)$$

The partial derivatives were evaluated using the expected (average) values of all quantities in the calculation. At the subwatershed exits, the variances $\sigma_{c_1}^2$ and $\sigma_{c_2}^2$ were derived from the pollutant EMCs per land use and $\sigma_{Q_1}^2$ and $\sigma_{Q_2}^2$ were determined using Equation 6. At the junctions, $\sigma_{c_1}^2$ and $\sigma_{c_2}^2$ were either derived from input pollutant data (discussed in a later section) or taken from upper stream segments depending on the watersheds intersecting at each junction. Similarly, $\sigma_{Q_1}^2$ and $\sigma_{Q_2}^2$ were determined from Equation 6. In cases where an upstream segment is present, the variance in concentration (not flow) was attenuated according to Equation 5, where c_a and c_u were replaced with the appropriate σ_c^2.

3. USGS Model

The UM model was compared with the USGS water-quality model as a reference point. The USGS model is described by (Chin 2006a):

$$Y = 0.454(N)(BCF)10^{[a+b\sqrt{(DA)}+c(IA)+d(MAR)+e(MJT)+f(X2)]} \quad (13)$$

where Y is the yearly pollutant load (kg), N is the average number of storms per year, BCF is a bias correction factor, DA is the total contributing drainage area (ha), IA is the impervious area as a percentage of the total contributing area (%), MAR is the mean annual rainfall (cm), MJT is the mean minimum January temperature (°C), $X2$ is an indicator variable related to land use, and the remaining parameters are shown in Table 1. The values used for this analysis were N = 70, IA = 30%, MJT = 16°C, and $X2$ = 1 if the urban area is greater than 75% of the contributing area and 0 otherwise. Parameters for the USGS model are available for the five pollutants shown in Table 1.

4. Model Parameters

4.1 Rainfall-Runoff Parameters

There is little available rainfall data in Cuba for runoff modeling. However, due to the close proximity of Havana to South Florida as shown in Figure 2, the validity of using rainfall data from South Florida as a surrogate for rainfall in Havana was investigated. A comparison of the monthly rainfall characteristics in Miami and Havana is shown in Figure 3 (www.climatetemp.info). These data show that Miami and Havana follow the same seasonal trends with peak rainfall amounts in June and September/October, wet seasons from March-September, and dry seasons from October-February. Additional climate data gathered included average annual temperature, average number of wet days per year (> 0.1 mm), average relative humidity, and average wind speed; these data are shown in Table 2 (www.climatetemp.info).

Table 1. USGS model parameters

Pollutant	*a*	*b*	*c*	*d*	*e*	*f*	BCF
TN	-0.2433	0.1018	0.0061	-	-	-0.4442	1.345
TP	-2.0700	0.1294	-	0.00921	-0.0383	-	1.314
Cu	-1.9336	0.1136	-	-	-0.0254	-	1.403
Pb	-1.9679	0.1183	0.0070	0.00504	-	-	1.365
Zn	-1.6302	0.1267	0.0072	-	-	-	1.322

Source: Taken from Chin (2006a)

Figure 2. Caribbean area

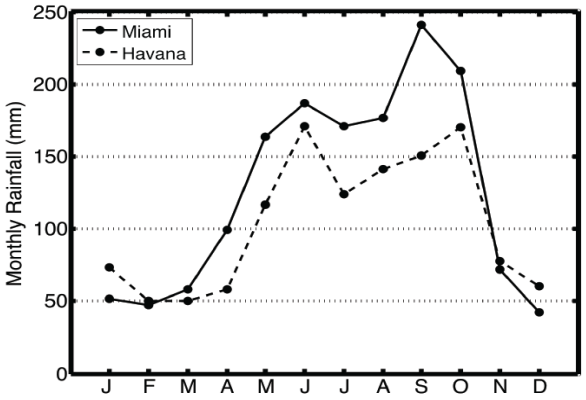

Figure 3. Comparison of monthly rainfall characteristics between Havana and Miami

Table 2. Climate comparison between Havana and Miami

	Avg. Temp (^{o}C)	Wet Days (> 0.1 mm)	Avg. Relative Humidity (%)	Avg. Windspeed (km/hr)
Miami	24	132	60.6	12-19
Havana	25	121	74.3	10-15

The analysis presented here was based on the average rainfall characteristics at several rainfall stations in South Florida, and the average annual rainfall at these stations is compared with that of Havana in Figure 4.

Note that the monthly data plotted for Miami and Havana in Figure 3 was taken from the same source (www.climatetemp.info) for purposes of comparison, while the data shown for the US stations in Figure 4 came from the National Climatic Data Center (NCDC) and the value for Havana came from a Cuban source (Hernández and Mon, 1996). The use of different sources to establish monthly rainfall patterns and yearly totals was necessary since the NCDC did not provide data for Havana. The use of different sources explains the differences in total rainfall, where Figure 3 shows Miami receiving more rainfall than Havana while Figure 4 shows Havana receiving more rainfall than Miami. The annual rainfall at the South Florida stations ranged from 1344 mm/year at St. Lucie New Lock 1 to 1485 mm/year at West Palm Beach International Airport as shown in Figure 4, which also shows that Havana averages 1411 mm/year, falling within the range of the five South Florida stations.

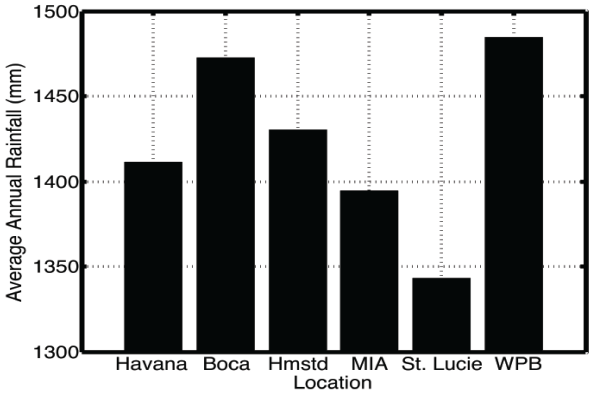

Figure 4. Comparison of Havana and South Florida rainfall used in calculating runoff coefficients

Using spatially-averaged hourly rainfall measurements in South Florida, Harper and Baker (2007) developed a table of runoff coefficients depending on the runoff properties of the land surface. The runoff coefficient, *C*, represents the ratio of annual runoff depth to the annual precipitation depth, described by

$$C = \frac{annual\ \ runoff\ \ (mm)}{annual\ \ rain\ fall\ (mm)} \qquad (14)$$

and is in the range [0-1.0]. The *C* values reflect the average runoff/rainfall ratio for a given meteorological monitoring site over the entire available period of record, which was typically 30 years or more for the stations used by Harper and Baker (2007) to describe South Florida rainfall (see Figure 4). The runoff coefficients were determined as a function of curve number (CN) and directly-connected impervious area (DCIA), where CN is a widely used parameter for predicting direct runoff for various soil conditions and land uses, and DCIA refers to those areas that are in direct hydraulic connection to the conveyance system (i.e. storm drains) without flow over pervious areas or infiltration into the ground. The UM model was set up such that urban and non-urban land uses were characterized by CN ranges of 85-98 and 60-75, respectively, and by DCIA ranges of 65-85% and 0-15%, respectively, and the corresponding *C* values are shown in Tables 3a and 3b. The ranges of CN and DCIA selected were assumed to be representative of land types and land uses in the Almendares watershed and were used to determine the mean and standard deviation of the runoff coefficient used in the concentration predictions and uncertainty analysis of water quality in the watershed. The average yearly rainfall for Havana, *R*,

was assumed to be 1411 mm.

Table 3a. Runoff coefficient versus Curve Number and DCIA in urban areas

	DCIA					
CN		65	70	75	80	85
	85	0.598	0.628	0.658	0.688	0.718
	90	0.627	0.653	0.679	0.705	0.731
	95	0.681	0.699	0.717	0.736	0.754
	98	0.740	0.750	0.760	0.769	0.779

Table 3b. Runoff coefficient versus Curve Number and DCIA in non-urban areas

	DCIA				
CN		0	5	10	15
	60	0.057	0.095	0.132	0.170
	65	0.073	0.110	0.147	0.183
	70	0.093	0.129	0.165	0.201
	75	0.120	0.155	0.189	0.223

4.2 Land Uses

An up-to-date digital map with shape file data for Havana was not available, so the most recent digital map was used. The map was derived from the WGS1984 data set with the latest revision circa 2004. This is the most recent revision of the World Geodetic Systems reference frame for the Earth and is the standard for both cartography and navigation.

The Havana area is referenced in the WGS1984 Zone 17 North data set, which is bound by the Northern hemisphere and stretches from 84°W to 78°W on the world map. A standard spatial reference frame is then created for the Earth's surface and allows for area measurements to be calculated within ArcGIS. A resolution of 1:6000 was chosen for the analysis as a balance between the amount of area to be analyzed and the ability to determine the landscape and land use in the watershed. The watershed boundary was estimated via interpolation from a digital elevation map. Using ArcGIS 10, all visible river and stream segments within the watershed at a resolution of 1:6000 were mapped as polylines.

The sub-watershed boundaries are identified in Figure 5. Sub-watersheds for all streams were subsequently delineated within the final watershed boundary based on identifiable stream segments in the Almendares River and its tributaries both upstream and downstream of the Ejército Rebelde Reservoir. A map from the Cuban Heritage Collection at the University of Miami was also used as a reference for stream location and watershed boundaries (University of Miami, Cuban Map Collection).

Land areas were mapped as polygons within each digitally-created sub-watershed, and land uses within each sub-watershed were visually classified as either urban or non-urban areas. Urban areas, shown in white, represent developed lands used for both residential and commercial purposes, while non-urban areas shown in green represent farmlands, forests, undeveloped land, or areas where expanses of row crops could clearly be seen from the satellite image (see Figure 5). The field calculator within ArcGIS 10 was used to calculate area values of each individual urban or non-urban polygon as well as each stream polyline. These values were then summed corresponding to each respective sub-watershed for use in the water-quality model.

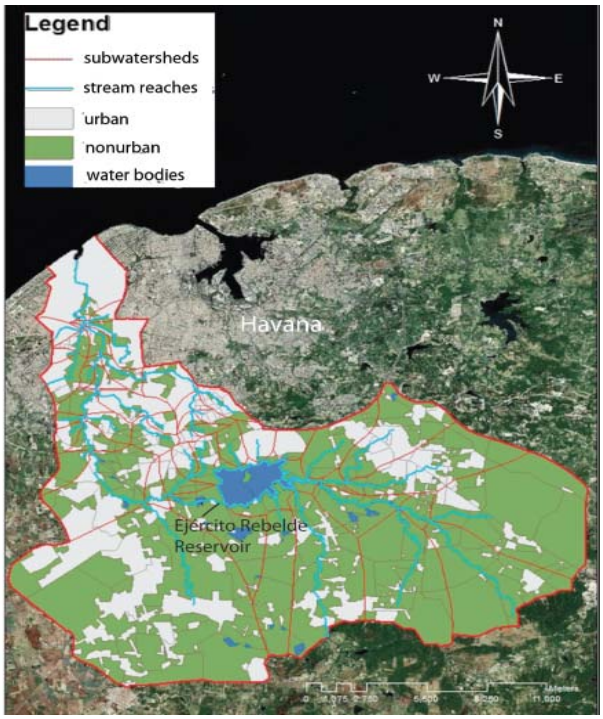

Figure 5. Map of the Almendares River watershed

4.3 Event-Mean Concentrations (EMCs)

The event-mean concentration is defined as the average mass of pollutant per unit volume of runoff. Pollutants often characterized by EMCs are heavy metals, five-day BOD, total suspended solids, total nitrogen, total phosphorus, soluble species of nitrogen and phosphorus, and indicators of pathogenic bacteria such as fecal coliforms and *E. coli*. The eight pollutants commonly found in stormwater runoff that were selected for inclusion in this study were: five-day BOD (BOD_5), total nitrogen (TN), total phosphorus (TP), Lead (Pb), Copper (Cu), Zinc (Zn), Cadmium (Cd), and fecal coliform (FC). One previous study examined some of these constituents in riverbed sediment of the Almendares River (Olivares-Rieumont et al., 2005), however the focus of the present study is contaminants contained in the stream flow rather than in the sediment.

Published EMC data for Cuba were unavailable. However, since land use is the primary factor in

determining EMCs, available EMC data from the United States was used (Chin, 2006b; Gain, 1996; Keith and Schnars, 2007; Migliaccio and Castro, 2009; FDEP, 2010). The published EMCs were organized by land use, varying from "mixed" or "urban" to "religious facilities" and "transportation". For the purpose of the current study, land uses were considered as either urban or non-urban, and the values for each pollutant were combined to determine a mean, standard deviation, and coefficient of variation of the EMC.

An example of the EMC data for lead (Pb) is illustrated in Figure 6 for both urban and non-urban land uses. The Gaussian distribution shown was calculated from the mean and standard deviation for Pb in each land use taken from the National Urban Runoff Project (NURP) (Chin, 2006b). The distributions shown contain four standard deviations greater than and less than the mean. For each concentration value, the probability density was calculated using the normal distribution. Figure 6a and 6b depict the urban and non-urban EMC distributions, respectively.

The individual points on the abscissa of each graph are all values from the individual EMC sources used in this study. The relative size of these points on the axis denotes the number of sources that had the same EMC value for the constituent. Comparing the individual EMC results with the statistical results of the NURP data, it is apparent that there are some outliers on both the upper and lower ends. However many of the data points are inside the curve, and the mean of the data is within the range of the probability distribution of the NURP data. This same analysis was performed for the eight pollutants considered in this study, and the majority of data points from individual studies were found to be within the Gaussian distribution fitted to the NURP data.

The available EMC data for each contaminant/land-use scenario were combined to determine an overall mean and standard deviation of the EMC for the given scenario. The results of these calculations are shown in Table 4. Each data point was given equal weight. In the case of non-urban FC, there was only one data point, so there is no standard deviation or COV.

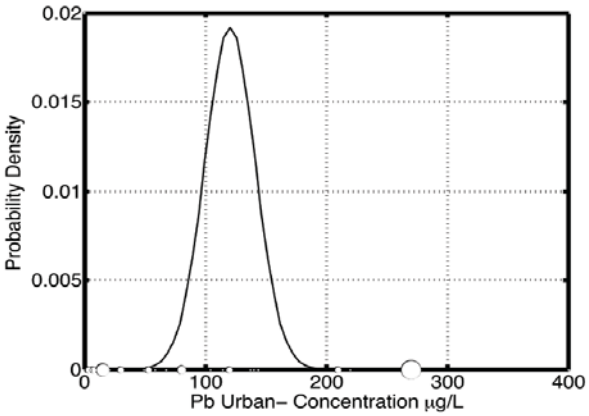

Figure 6a. Urban EMC distributions

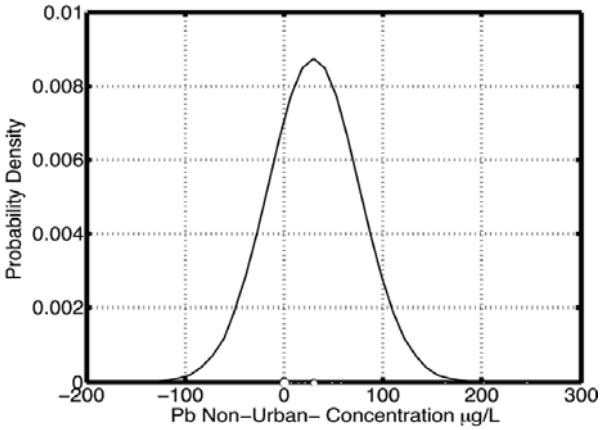

Figure 6b. Non-urban EMC distributions

Table 4. Event-mean concentrations and water-quality standards

	Urban Land		Non-Urban Land		Florida Standard
	Mean	Std Deviation	Mean	Std Deviation	
BOD_5 (mg/L)	10.90	5.77	3.03	3.22	-
TN (mg/L)	1.64	0.45	1.77	0.83	-
TP (mg/L)	0.30	0.26	0.36	0.39	-
Pb (μg/L)	97.7	104.0	55.4	80.0	9.6
Cu (μg/L)	33.0	33.9	44.5	35.2	16.7
Zn (μg/L)	349.8	1239.6	168.5	202.4	212.0
Cd (μg/L)	6.7	8.4	1.7	2.5	0.4
Fecal coliform (CFU/dL)	3000	1100	2300	-	200

4.4 Water-Quality Standards

The State of Florida water-quality standards were used as a basis for assessing water quality in the streams of Havana (FDEP, 2010). Water-quality standards are available for five different designated water uses (Class I to Class V), and Class III standards were applied in this study. The designated uses of Class III waters are: fish consumption, recreation, propagation and maintenance

of a healthy, well-balanced population of fish and wildlife. Class III has two subcategories: primarily fresh waters and primarily marine waters; the fresh water standards were used in this study.

There are currently no numeric water-quality standards for BOD_5, TN, or TP in Florida. For the four heavy metals (Pb, Cu, Zn, Cd), the standards are determined by an equation that is a function of the hardness of the water. The equation uses a hardness value of 25 mg/L for any hardness less than 25 mg/L, a hardness value of 400 mg/L for any hardness greater than 400 mg/L, and the actual hardness in the range 25-400 mg/L. Based on a study by the U.S. Geological Survey (Briggs and Ficke, 1977), a significant portion of Florida is in the same range of hardness (121-180 mg/L $CaCO_3$). In addition, the USGS study also analyzed the island of Puerto Rico, which was also found to be in the 121-180 mg/L range for hardness. For the purposes of this study, the water quality standards applied for the metals were the average of the values found using a hardness of 25 mg/L and 400 mg/L. This assumed similarity between Havana and South Florida is further justified since Havana, like South Florida, is underlain by a karst aquifer (Suckow, 2003).

5. Results and Discussion

Water-quality simulations were performed for all eight pollutants of concern. Most of the results showed similar patterns, and these results will be shown here in detail for lead (Pb) and summarized for the remainder of the pollutants. The water-quality predictions for concentrations of Pb with 90% confidence intervals (CI) in the stream junctions of the main stem of the Almendares River for upper and lower regions are shown in Figure 7a and 7b, respectively.

The junctions shown are for both the upper region (above the Ejército Rebelde reservoir) in Figure 7a, and for the lower region (below the Ejército Rebelde reservoir) in Figure 7b. The junctions plotted in Figure 7b are, from left to right, 119, 118, 117, 116, 115, 114, 113, 111, 110, 106, 103, 101, 100 (coast) and can be seen in Figure 8.

It was found that the relative distribution of concentrations at the stream junctions were similar for different pollutants, and primarily varied in scale depending on the mean and standard deviation of the EMC of each pollutant. In other words, the shape of the distribution of concentrations shown in Figure 7 was consistent for all pollutants, but the magnitude of the concentrations depended on the value of the EMCs. The distribution of the concentrations does not change because the modeled flows are a function of the runoff coefficients and the landscape, which do not change between pollutants. As a reference point in Figure 7 the Florida Class III water quality standard for Pb is also shown (9.6 µg/L), and it can be seen that five of the stream junctions in the lower region and all three junctions in the upper region violate this water-quality standard.

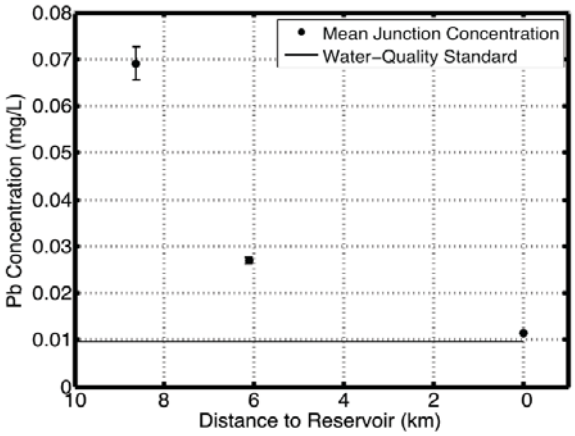

Figure 7a. Runoff model junction concentrations with 90% CI for Pb in upper region

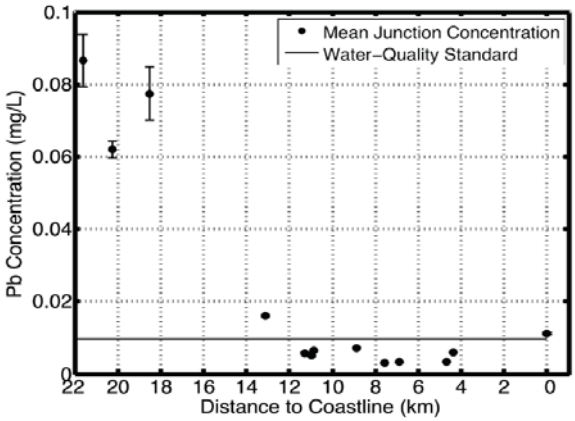

Figure 7b. Runoff model junction concentrations with 90% CI for Pb in lower region

In the lower region of the Almendares River watershed, the locations of the three highest junction concentrations (119, 118, 117) all occur farthest upstream while the average concentration decreases downstream approaching the coastline. Although the coastal areas are highly urbanized and therefore more susceptible to contamination by surface runoff, the lower concentrations that are found in the lower reaches of the Almendares River are likely due to dilution from greater flows and from attenuation over the river distance travelled.

Moreover, the predicted concentrations at the three most-upstream junctions are close to the pollutant EMC values listed in Table 4. This pattern was repeated at four other junction locations (102, 105, 109, and 112) which are not located on the main river stem but are shown in relation to the main stem in Figure 8. Each of these

junctions represents the union of two individual sub-watersheds without contribution from upstream segments, and the predicted concentrations at these junctions are near the EMC values. This result further demonstrates that junctions of upper sub-watersheds are most likely to violate water-quality standards, regardless of proximity to the coast or urban/non-urban land-use distribution, and that dilution and attenuation serve to reduce concentrations downstream after the summing of flow from several junctions.

Figure 8. Stream junctions in the Lower Almendares River watershed

The only way to reduce concentrations to meet water-quality standards is to reduce the EMC via better management of sub-watershed runoff. An example of such action in both upper and lower regions can be seen in Figures 9a and 9b, where the urban and non-urban EMC for Pb were reduced to 9.6 µg/L from 97.7 µg/L and 55.4 µg/L, respectively. The reduction in EMC was shown to produce mean junction concentrations that do not violate the water quality standard.

The assumption that contaminant attenuation in streams could be characterized by K = 1,000 m^{-1} as assumed in Figure 7 was examined to better understand the sensitivity of the results to the assumed attenuation factor. This sensitivity was investigated by using the UM model with K = 100 m^{-1} and K = 10000 m^{-1}, which yielded the results shown in Figure 10a and 10b, respectively. It can be seen that K values of 100 m^{-1} and 1000 m^{-1} produced little change in the shape and scale of the distribution of the average concentrations. Using a value of K = 10,000 m^{-1}, however, created more noticeable changes in the shape and scale of the distribution. The most important observation is that the junctions with the most severe water-quality violations do not change as K varies, thereby justifying the use of K = 1,000 m^{-1}.

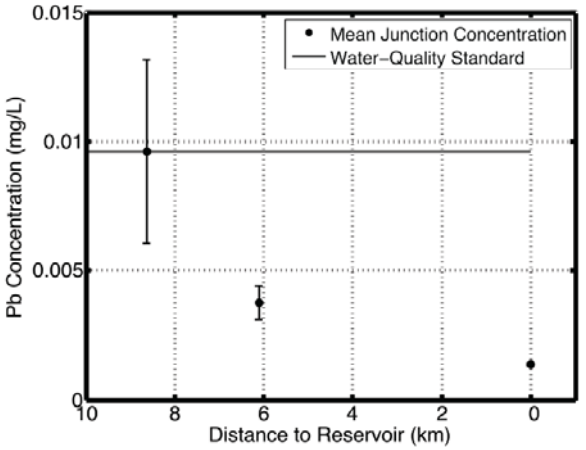

Figure 9a. Reduced Pb EMCs produce zero water-quality impairments in upper region

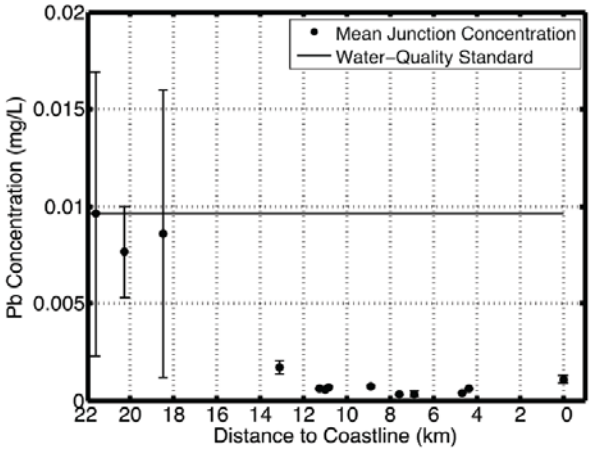

Figure 9b. Reduced Pb EMCs produce zero water-quality impairments in lower region

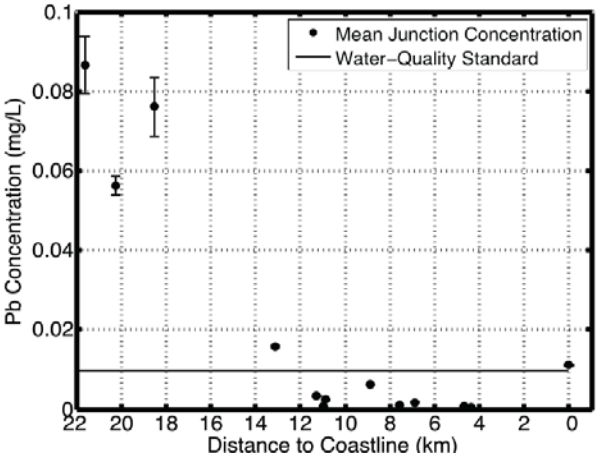

Figure 10a. Pb concentrations for attenuation factor, K = 100m^{-1}

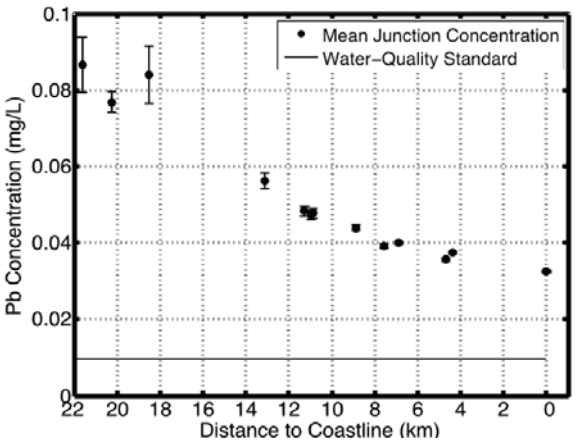

Figure 10b. Pb concentrations for attenuation factor, K = 10,000 m^{-1}

The contaminant loads in both upper and lower regions predicted by the UM model are compared to the contaminant loads predicted by the USGS model in Figures 11a and 11b, respectively.

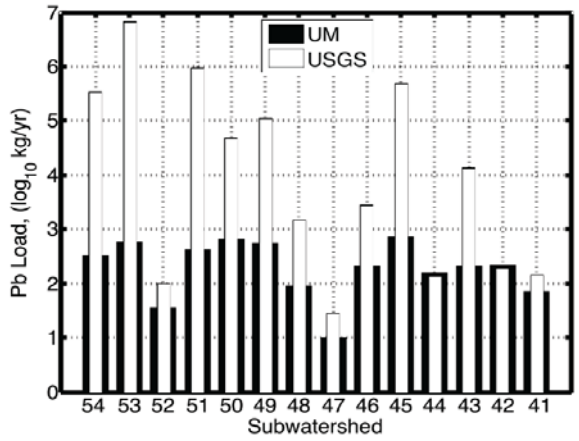

Figure 11a. Comparison of predicted loads in upper region using UM model and USGS model

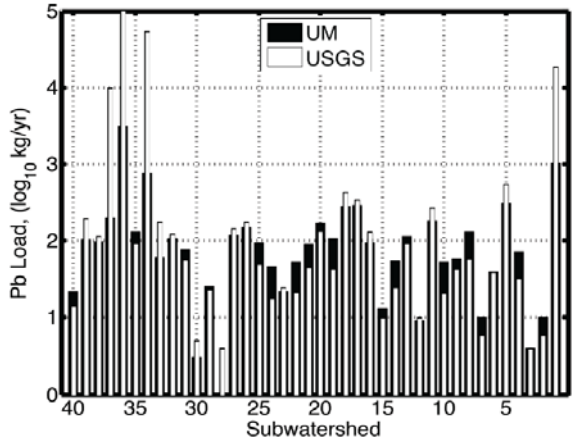

Figure 11a. Comparison of predicted loads in lower region using UM model and USGS model

Based on these results, it is apparent that the difference between the USGS and UM model depends on sub-watershed land area; the range of areas in the upper and lower region are 80-2972 ha and 2-7571 ha, respectively. The UM model yielded contaminant loads comparable to the USGS model for sub-watersheds with areas roughly in the middle of the range of areas, such as sub-watersheds 41 (224 ha), 42 (257 ha), and 44 (221 ha) in the upper region and sub-watersheds 6 (107 ha), 26 (250 ha), and 31 (134 ha) in the lower region. However, in the two largest sub-watersheds in the upper and lower regions, 53 (2972 ha), 51 (2237 ha), 36 (7571 ha) and 34 (1348 ha), respectively, the USGS models predicted loads that were several orders of magnitude larger than the UM model.

Similarly, the two smallest sub-watersheds in the upper and lower regions, 47 (80 ha), 52 (184 ha), 28 (2 ha), and 3 (4 ha), respectively, had the smallest magnitude of USGS loads. This is likely due to the fact that the USGS model (Equation 13) has the land-area term *DA* in the exponent of the equation, therefore increasing its sensitivity in the overall model output. The USGS model predicted greater loads than the UM model in most sub-watersheds in the upper region while the greater load was roughly split between the models in the sub-watersheds of the lower region.

All of the results presented in detail were for Pb, because it was applicable in the USGS model and because Class III water-quality standards were available. Table 5 shows a summary of the other pollutants considered with available water-quality standards, where the number of junctions with predicted concentrations that exceeded the water-quality standard is provided.

Table 5. Water-quality results for all contaminants

Pollutant	FC	Pb	Cu	Zn	Cd	FC
Lower Region (# of exceedances)	7	5	3	2	6	7
Upper Region (# of exceedances)	3	3	1	1	3	3

The main stems in the lower and upper regions incorporated 13 and 3 junctions, respectively. The top-three locations with most serious water-quality violations for Pb were also the top-three locations where violations of water-quality standards by the other constituents are expected to occur.

Finally, the methodology presented in this paper for developing a model is unorthodox and needs to be evaluated objectively. The main hindrance in the model development was the lack of available data from the Almendares watershed, which is not an uncommon problem and unfortunately is not a problem that is likely to be amended anytime soon. For example, an author from the Olivares-Rieumont et al. (2005) paper informed us that some streamflow records do exist, but are

recorded on paper and stored in filing cabinets in buildings of the Cuban government and are therefore extremely difficult to access (DW Graham, personal communication, September 29, 2011).

However, modeling strategies like the one employed here, which comprehensively account for uncertainty in model equations, model parameters, and model outputs, present a viable option. It is likely that much of the future development and reconstruction work in Cuba will be done by non-Cuban governments, non-profit agencies, and contractors, and our approach may be an attractive one for other analyses until a sufficient database has been developed specific to Cuba. While the topography of the Almendares watershed features notably more elevation changes compared to the relatively flat landscape of South Florida and is an issue that will need to be dealt with better in the future, the other factors such as weather patterns, land use, and land cover are similar enough in the two regions to allow the implementation of data from one region to the other, even across political boundaries. In the big picture, we acknowledge that our approach is not ideal, but feel it is a sufficient first step towards addressing water-quality issues in Cuba and has many promising future applications.

6. Conclusions

The model presented is an attempt to link land uses and water quality in the upper and lower regions of the Almendares River watershed. The model used a GIS platform to divide the watershed into urban and non-urban land uses, and assigned runoff coefficients and EMCs for selected pollutants to each land-use type. Because water-quality data and standards in Cuba were unavailable, the required data and standards were taken from the state of Florida, an approach justified by the highly correlated meteorological patterns between South Florida and Havana. While point-source pollution exists in the watershed, the model did not consider these sources due to a lack of data and a focus on the relationship between land use and water quality. The model only considered pollutant contributions from runoff and surface waters and did not consider groundwater interaction. In neglecting point sources and groundwater, however, the model presents a conservative assessment for analyzing the relationship between land use and water quality in the watershed.

Given the assumptions used to build the model, the results showed that the river junctions with the highest probability of exceeding the water-quality standards are at the intersections of upstream sub-watersheds. This result was found to be true regardless of the land uses within the sub-watersheds or the location of the sub-watersheds within the greater Almendares watershed, indicating that dilution and attenuation combine to reduce pollutant concentrations at downstream river junctions. The junctions of concern had average concentrations near the EMC values assigned to the land uses, indicating that the only way to mitigate the high junction concentrations is to reduce the EMCs by better management of the surface runoff in the upstream sub-watersheds. Attenuation factors over three orders of magnitude were considered, and while the magnitude of the average concentration at some junctions fluctuated, the junctions of concern were the same at all attenuation factors evaluated. Finally, the model was found comparable to an established USGS water-quality model.

This study developed a simple yet effective model to provide a relative assessment of the water quality in the Almendares River watershed in Cuba. The model is a first step in addressing water quality in the Almendares River, and its most significant contribution is the identification of river junctions of concern in the watershed where initial remediation efforts should be directed. The methodology used to develop the model accounts for uncertainty in the model equations, model parameters, and model outputs, and is particularly useful in areas such as Cuba with limited data. The model can be a useful analysis tool in the present and in the future, in both the Almendares River and other parts of Cuba, as more engineering data becomes available and as Cuba addresses the state of its water resources and environment.

References:

Benjamin, J.R. and Cornell, C.A. (1970), *Probability, Statistics, and Decision for Civil Engineers*, McGraw-Hill, New York.

Briggs, J.C., and Ficke, J.F., (1977) "Quality of Rivers of the United States, 1975 Water Year - Based on the National Stream Quality Accounting Network (NASQAN)", *U.S. Geological Survey Open-File Report 78-200*, 436 p.

Climatetemp (2012), *World Weather and Climate Graphs, Average Climate Charts, Guide to Precipitation, Temperatures, Best, Friendly, Holiday Climate*, available at http://www.climatetemp.info, <Accessed: December 2012>

Chin D.A, (2006a), *Water-Resources Engineering, 2nd Edition,* Pearson Prentice Hall, New Jersey.

Chin, D.A., (2006b) *Water-Quality Engineering in Natural Systems*, John Wiley and Sons, Hoboken, New Jersey.

Egues R.A. and Diaz, J.G. (1997), "Saneamiento de la Cuenca Almendares", *Emp. Inv. Proy. Hid. Habana Humboldt y P # 106*, Vedado. Ciudad de La Habana, Cuba.

Florida Department of Environmental Protection (2010), *Surface Water Quality Standards. Tech. No. 62-302.530*. 45th Edition, Vol.37, Florida Administrative Weekly and Florida Administrative Code.

Gain, S.W. (1996), *The Effects of Flow-Path Modification on Water-Quality Constituent Retention in an Urban Stormwater Detention Pond and Wetland System, Orlando, Florida*, Report Number 95-4297, U.S. Geological Survey.

Harper, H.H. and Baker, D.M. (2007), *Evaluation of Current Stormwater Design Criteria within the State of Florida*, Florida Department of Environmental Protection.

Hernández, A.J.L. and Mon, E.A. (1996), "Caracterización del Abastecimiento de Agua Potable y Saneamiento de la Ciudad de La Habana", *Emp. Inv. Proy. Hid. Habana Humboldt y P # 106*. Vedado. Ciudad de La Habana, Cuba.

Keith and Schnars, P.A. (2007), *South Miami-Dade Watershed Study and Plan*. Publication. Miami-Dade County Department of Environmental Resources Management, March

(http://southmiamidadewatershed.net/).

Migliaccio, K., and Castro, B. (2009), *Storm Event Sampling in Biscayne Bay Watershed*, Final Project Report, South Florida Water Management District.

Olivares-Rieumont S, de la Rosa, D., Lima, L., Graham, D.W., D'Alessandro, K., Borroto, J., Martinez, F. and Sanchez, J. (2005), "Assessment of heavy metal levels in Almendares River sediments- Havana City, Cuba", *Water Research*, Vol.39, pp.3945-3953.

Suckow, A. (2003), *An Integrated Geological, Geophysical, Geochemical and Isotope Hydrological Approach to Study the Marine–Ground Water Interaction*, Report No. IAEA-CN-104/P-76. Leibniz Institute for Applied Geosciences (GGA), Hannover, Germany, Department of Geophysics and Astronomy, May.

University of Miami (n.d.), *Cuban Map Collection. Croquis de la Provincia de La Habana. 1:200,000*, Cuban Heritage Collection, tray 38, folder 25, item 108.

Authors' Biographical Notes:

Jeffrey J. Iudicello *is a former graduate student in Civil Engineering at the University of Miami. He is currently a Water Resources Engineer / Modeler with the Delaware River Basin Commission, West Trenton, NJ.*

Dylan A. Batterman *is a former undergraduate student in Environmental Engineering at the University of Miami. He is currently pursuing a career in project and environmental engineering*

Matthew M. Pollard *is a former undergraduate student in Environmental Engineering at the University of Miami. He is currently pursuing a graduate degree in Chemical and Environmental Engineering from Washington University in St. Louis, MO.*

Cameron Q. Scheid *is a former undergraduate student in Environmental Engineering at the University of Miami. He is currently pursuing a career in environmental engineering.*

David A. Chin *is a Professor in the Department of Civil, Architectural, and Environmental Engineering, University of Miami, Coral Gables, FL.*

■